Mass cytometry reveals single-cell kinetics of cytotoxic lymphocyte evolution in CMV-infected renal transplant patients

Kenichi Ishiyama[a,b], Janice Arakawa-Hoyt[a,b], Oscar A. Aguilar[a,b], Izabella Damm[c], Parhom Towfighi[c], Tara Sigdel[c], Stanley Tamaki[d], Joel Babdor[a,b,e], Matthew H. Spitzer[a,b,e,f], Elaine F. Reed[g], Minnie M. Sarwal[c], Lewis L. Lanier[a,b,1], and CMV Systems Immunobiology Group

[a]Department of Microbiology and Immunology, University of California, San Francisco, CA 94143; [b]Parker Institute for Cancer Immunotherapy, University of California, San Francisco, CA 94143; [c]Department of Surgery, University of California, San Francisco, CA 94143; [d]Parnassus Flow Cytometry Core, University of California, San Francisco, CA 94143; [e]Department of Otolaryngology–Head and Neck Surgery, University of California, San Francisco, CA 94143; [f]Chan Zuckerberg Biohub, San Francisco, CA 94158; and [g]Department of Pathology and Laboratory Medicine, University of California, Los Angeles, CA 90095

Contributed by Lewis L. Lanier; received September 8, 2021; accepted January 5, 2022; reviewed by Katharine Hsu and Sungjin Kim

Cytomegalovirus (CMV) infection is associated with graft rejection in renal transplantation. Memory-like natural killer (NK) cells expressing NKG2C and lacking FcεRIγ are established during CMV infection. Additionally, CD8$^+$ T cells expressing NKG2C have been observed in some CMV-seropositive patients. However, in vivo kinetics detailing the development and differentiation of these lymphocyte subsets during CMV infection remain limited. Here, we interrogated the in vivo kinetics of lymphocytes in CMV-infected renal transplant patients using longitudinal samples compared with those of nonviremic (NV) patients. Recipient CMV-seropositive (R+) patients had preexisting memory-like NK cells (NKG2C$^+$CD57$^+$FcεRIγ$^-$) at baseline, which decreased in the periphery immediately after transplantation in both viremic and NV patients. We identified a subset of prememory-like NK cells (NKG2C$^+$CD57$^+$FcεRIγ$^{low–dim}$) that increased during viremia in R+ viremic patients. These cells showed a higher cytotoxic profile than preexisting memory-like NK cells with transient up-regulation of FcεRIγ and Ki67 expression at the acute phase, with the subsequent accumulation of new memory-like NK cells at later phases of viremia. Furthermore, cytotoxic NKG2C$^+$CD8$^+$ T cells and γδ T cells significantly increased in viremic patients but not in NV patients. These three different cytotoxic cells combinatorially responded to viremia, showing a relatively early response in R+ viremic patients compared with recipient CMV-seronegative viremic patients. All viremic patients, except one, overcame viremia and did not experience graft rejection. These data provide insights into the in vivo dynamics and interplay of cytotoxic lymphocytes responding to CMV viremia, which are potentially linked with control of CMV viremia to prevent graft rejection.

NK cell | renal transplantation | cytomegalovirus | mass cytometry | cytotoxic lymphocyte

Cytomegalovirus (CMV) is life threatening for individuals with a compromised immune system, including solid organ and hematopoietic stem cell transplant patients. Additionally, infection or reactivation of CMV resulting in viremia in solid organ transplant patients has been associated with chronic graft rejection (1, 2). Through constant surveillance, natural killer (NK) and T cells cooperatively control CMV throughout an individual's life. The antiviral drugs used prophylactically in transplant patients have significant side effects and toxicity, and there is no currently approved vaccine for CMV.

We and others have identified a subpopulation of NK cells bearing the activating CD94-NKG2C receptor that preferentially respond to acute CMV infection in both solid organ (3) and hematopoietic stem cell transplant recipients (4–6). These NKG2C$^+$ cells also express CD57, which marks a population of mature NK cells with a distinct phenotype and function (7, 8). These NKG2C$^+$CD57$^+$ NK cells are specific to CMV in that they do not respond to acute infection with Epstein–Barr virus during infectious mononucleosis (9) or herpes simplex virus (10). Moreover, these NK cells have been observed to be reactivated and persist over several years only in individuals who have been infected with CMV. These findings are in line with those from mouse models, in which Ly49H$^+$ NK cells specifically respond to CMV infection (11–13) and have memory-like signatures (14), suggesting that in humans, NKG2C$^+$CD57$^+$ NK cells could include subsets with memory-like properties. Within this CMV-specific NKG2C$^+$CD57$^+$ NK cell population, we identified a unique subset of NK cells that do not express the FcεRIγ signaling subunit, which is expressed by all naıve NK cells. Rather, these FcεRIγ$^-$ NK cells preferentially use the CD3ζ signaling adapter and ZAP70 tyrosine kinase for signal transduction mediated by the CD16 Fc receptor. These NK cells exhibit robust preferential expansion and an enhanced antibody-dependent cellular cytotoxicity (ADCC) response

Significance

Memory-like NK cells (NKG2C$^+$CD57$^+$FcεRIγ$^-$) are established during CMV infection. Here, mass cytometry tracked the in vivo kinetics of CMV-induced memory NK cells generation and identified a unique subset of NKG2C$^+$CD57$^+$FcεRIγ$^{low–dim}$ as potentially prememory-like NK cells in CMV-infected kidney transplant patients. The study demonstrated that prememory-like NK cells with a high cytotoxic profile proliferate along with accumulation of new memory-like NK cells, whereas preexisting memory-like NK cells decreased in the peripheral blood after transplantation. Moreover, NKG2C$^+$CD8$^+$ T cells and cytotoxic γδ T cells also expand during CMV infection. This interplay of three different cytotoxic lymphocytes demonstrates a combinatorial immune response against CMV infection, which may contribute to preventing CMV-associated complication in organ transplantation.

Author contributions: K.I., E.F.R., M.M.S., L.L.L., and C.S.I.G. designed research; K.I., J.A.-H., O.A.A., I.D., P.T., and T.S. performed research; S.T., J.B., and M.H.S. contributed new reagents/analytic tools; K.I. analyzed data; I.D., P.T., and T.S. managed clinical samples and clinical data; and K.I. and L.L.L. wrote the paper.

Reviewers: K.H., Memorial Sloan Kettering Cancer Center; and S.K., University of California Davis.

The authors declare no competing interest.

A complete list of the CMV Systems Immunobiology Group can be found in the *SI Appendix*.

[1]To whom correspondence may be addressed. Email: lewis.lanier@ucsf.edu.

This article contains supporting information online at http://www.pnas.org/lookup/suppl/doi:10.1073/pnas.2116588119/-/DCSupplemental.

Published February 18, 2022.

against CMV-infected cells in an antibody-dependent manner (15–17). In addition to NK cells, minor subsets of $CD3^+$ T cells and γδ T cells, which express natural killer cell receptors (NKRs), are observed preferentially in CMV-seropositive patients (18, 19). Although such different lymphocyte subsets have been associated with immune response to CMV infection (20), in vivo kinetics of these immune-competent subsets over CMV infection remain limited.

The aims of this study were to determine how specific subsets of human NK cells respond to CMV infection or reactivation in solid organ transplant recipients and to demonstrate the dynamic interactions between NK cells and T cells responding to CMV viremia in the same transplant patients. For this, we used mass cytometry to longitudinally analyze peripheral blood mononuclear cells (PBMCs) from renal transplant patients who underwent CMV infection or reactivation, followed by single-cell data analysis using clustering methods. Notably, our panel included markers such as NKG2C, CD57, FcεRIγ, Syk, and inhibitory killer cell immunoglobulin-like receptors (KIRs) for the purpose of in-depth phenotyping of the responding NK cells and T cells. This enabled us to identify different NK cell subsets, including memory-like NK subsets, to define the in vivo kinetics of the NK cell response over CMV infection at the single-cell level. Moreover, our study identified minor populations of cytotoxic T cells responding to CMV viremia and demonstrated the interplay between NK cells and T cells during CMV viremia. This study provides insights into how these immune-competent cells respond to CMV infection in vivo, may contribute to host protection, and potentially, influence graft survival.

Results

Kinetic Change of Lymphocyte Subsets in CMV Infection. We examined longitudinal changes in PBMC subsets in kidney transplant patients with CMV infection or reactivation at four or five time points, with samples collected at day 0 of transplantation; at a time point prior to viremia; and then, postviremia at ∼1 wk, ∼1 mo, and long term (>1 mo). Matched control kidney transplantation patients without CMV viremia (nonviremic [NV]) were evaluated at three time points (day 0 and at approximately days 50 [median 51] and 180 [median 183] post-transplant) (Fig. 1). Patients in both groups showed that absolute counts of all lymphocyte subsets decreased at the second time point after transplantation (Fig. 2 and *SI Appendix*, Fig. S1), likely because of lymphopenia caused by immunosuppressive agents and CMV prophylactic drugs. Absolute counts as well as frequencies of NK cells, $CD8^+$ αβ T cells, and γδ T cells increased during the time course in viremic patients, whereas NV patients showed no significant changes (Fig. 2). $CD4^+$ T cells were stable in both groups, except for a transient increase at 1 mo in viremic patients (*SI Appendix*, Fig. S1). Frequencies and absolute counts of monocytes decreased in viremic patients but were stable in NV patients. These data suggest that viremic patients show dynamic changes of cytotoxic lymphocytes over CMV viremia.

NK Cell Subset Analysis in CMV-Seropositive Kidney Recipients. Prior studies have established that NK cells subsets are affected by prior CMV infection (18); therefore, we divided the cohort into two groups based on recipient CMV serostatus and performed an in-depth analysis of their NK cell repertoire using high-dimensional mass cytometry. NK cells were identified by the phenotype $CD3^-CD4^-CD14^-CD56^+$ cells. t-distributed stochastic neighor embedding (t-SNE) dimensionality reduction showed that recipient CMV-seropositive (R+) patients mainly have six NK subsets based on the NK cell marker panel (Fig. 3*A* and *SI Appendix*, Fig. S2). NKG2C, CD57, FcεRIγ, and CD2 expressions were the predominant drivers of the variance. CD57 expression was clearly distributed, defining the maturity axis. $CD57^-$ cells included $NKG2C^+CD57^-$ cells and immature NK cells, which were identified as $NKG2C^-CD57^-NKp30^+$ $NKp46^+$ cells regardless of CD2 expression. $CD57^+$ cells included four representative subsets. As FcεRIγ is a key marker to define functionally distinct types of $NKG2C^+CD57^+$ NK cells (15–17), we designated the $NKG2C^+CD57^+$ subsets characterized by $FcεRIγ^-$ as memory like and $FcεRIγ^{low\ to\ dim}$ as transitional prememory-like NK cells (although further studies

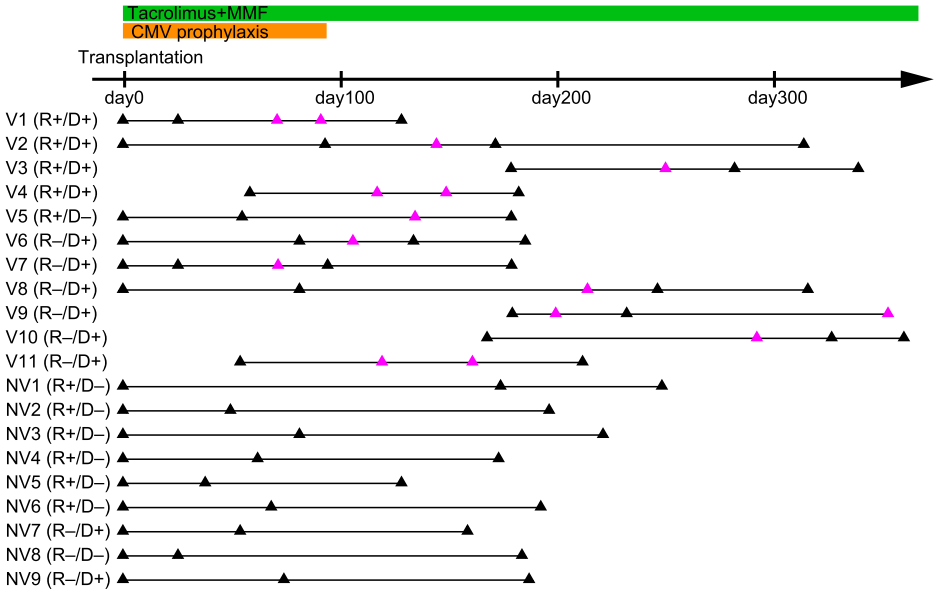

Fig. 1. Timetable of blood sampling. Time points of blood sampling (triangles) are shown. A pink triangle indicates detection of CMV viremia by PCR. Viremic patients had four or five sampling time points (day 0 of transplantation, previremia, ∼1 wk, ∼1 mo, and late [>1 mo] postviremia). NV patients had three sampling time points (day 0 and 50 and 180 d posttransplant). Viremic patients (n = 11) and NV patients (n = 9) used for longitudinal analysis are described. CMV serostatus in recipient (R) and donor (D) is shown. An R–/D– patient was not on CMV prophylaxis medication. V, viremic patient; MMF, mycophenolate mofetil.

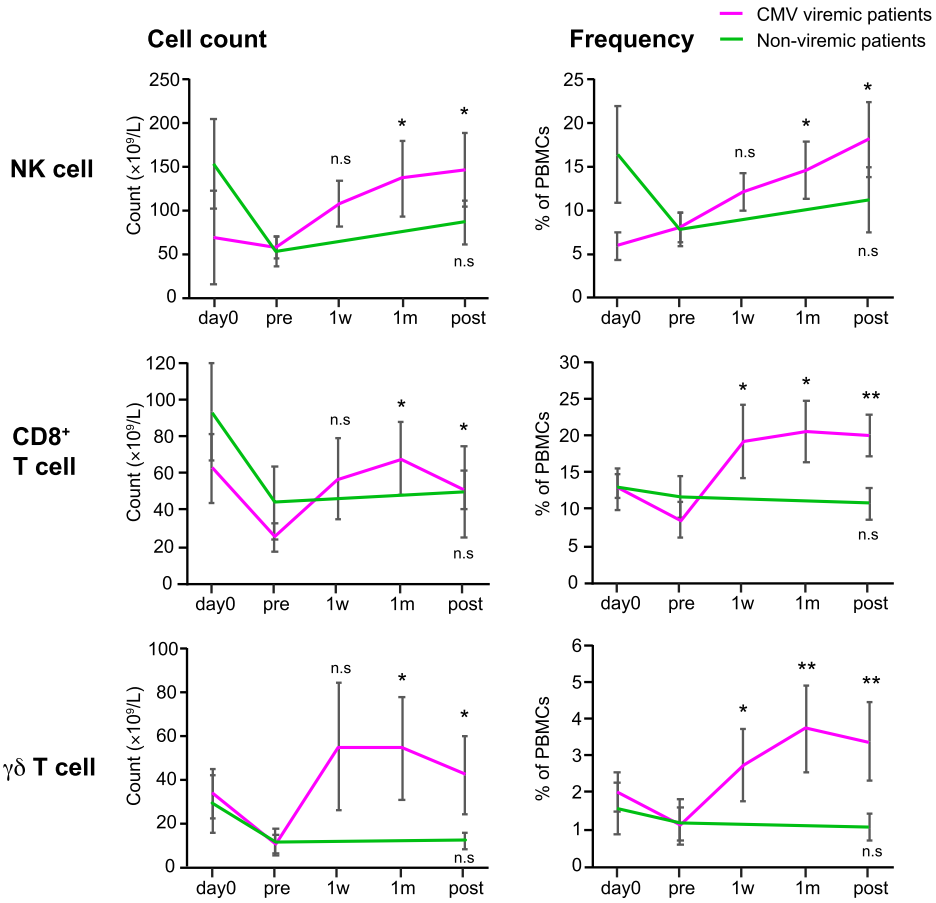

Fig. 2. Longitudinal changes of count and frequency of each lymphocyte subset in CMV infection. The *x* axis indicates time points. The *y* axis indicates count or frequency of each lymphocyte subset. Data at days 50 and 180 in NV patients were plotted at pre- and postviremia time points in viremic patients, respectively. Data represent the average count or percentage ± SEM from CMV viremic patients (pink, $n = 11$) and NV patients (green, $n = 9$). Statistical significance was analyzed with the Student's *t* test, relative to the previremia time point. n.s., not significant. $*P < 0.05$; $**P < 0.01$.

will be necessary to definitively demonstrate a precursor–product relationship of the "prememory" and "memory-like" NK cells) (Fig. 3). In addition, $NKG2C^{-}CD57^{+}$ cells and $CD57^{+}CD2^{-}$ cells were distinguished from the memory subsets. Thus, we determined longitudinal changes of six NK cell subsets (memory like, prememory like, mature $FcεRIγ^{+}NKG2C^{-}CD57^{+}$, $CD57^{+}CD2^{-}$, $NKG2C^{+}CD57^{-}$, and immature) in R+ patients. The frequency of preexisting memory-like NK cells decreased after transplantation in both viremic and NV patients (red in Fig. 3 *B* and *C*). Reciprocally, immature NK cells significantly increased in both groups (gray in Fig. 3 *B* and *C*). Intriguingly, the putative prememory-like NK cells significantly increased over the time course in viremic patients, whereas NV patients remained stable (green in Fig. 3 *B* and *C*). Moreover, t-SNE plots showed that $FcεRIγ^{-}$ prememory-like NK cells newly emerged and accumulated over viremia (Fig. 3 *C* and *D*), indicating the generation of new memory-like NK cells, which were observed exclusively in viremic patients and not in NV patients. To characterize the relationship among these three NK subsets with a memory-like phenotype, we examined Ki67 and FcεRIγ expression of single cells at postviremia time points. Prememory-like NK cells showed higher expression of Ki67 compared with memory-like NK cells in viremic patients, while there was no significant difference in NV patients (Fig. 3 *E* and *F*). Significant differences in Ki67 and FcεRIγ expression levels of newly generated memory-like NK cells were observed between the preexisting memory-like NK cells and newly generated prememory-like NK cells (Fig. 3 *E* and *F*). Furthermore, prememory-like NK cells as well as newly arising memory-like NK cells exhibited higher expression of cytotoxic effector molecules (granulysin, perforin, and granzyme B) compared with the preexisting memory-like NK cells (Fig. 3*G* and *SI Appendix*, Fig. S3). These data suggest that CMV viremia preferentially induced the proliferation of cytotoxic prememory-like NK cells along with accumulation of new memory-like NK cells. The expandability of preexisting memory-like NK cells appears lower than the newly generated prememory-like NK cells, depending on FcεRIγ expression. These findings are supported by the evidence that there is a significant positive correlation between Ki67 and FcεRIγ expression in viremic patients but not in NV patients (Fig. 3*E*). Longitudinal analysis of single cells showed Ki67 expression in all subsets, except that the preexisting memory-like NK cells were up-regulated at the previremia or ∼1-wk time point in viremic patients. FcεRIγ expression of prememory-like NK cells and immature NK cells was apparently up-regulated at the ∼1-wk time point compared with day 0, whereas there was no significant change in NV patients (Fig. 3*H*). These data suggest that CMV viremia transiently up-regulates FcεRIγ expression in NK cells, which is indicative of the enhanced proliferation capacity of NK cells.

NK Cell Subset Analysis in CMV-Seronegative Kidney Recipients. Studies were undertaken to determine if the kinetics and profile of alterations in the NK cell response would differ in CMV-seronegative (due to primary CMV infection) and CMV-seropositive (presumably reactivation of CMV) kidney transplant recipients. t-SNE dimensionality reduction identified several NK

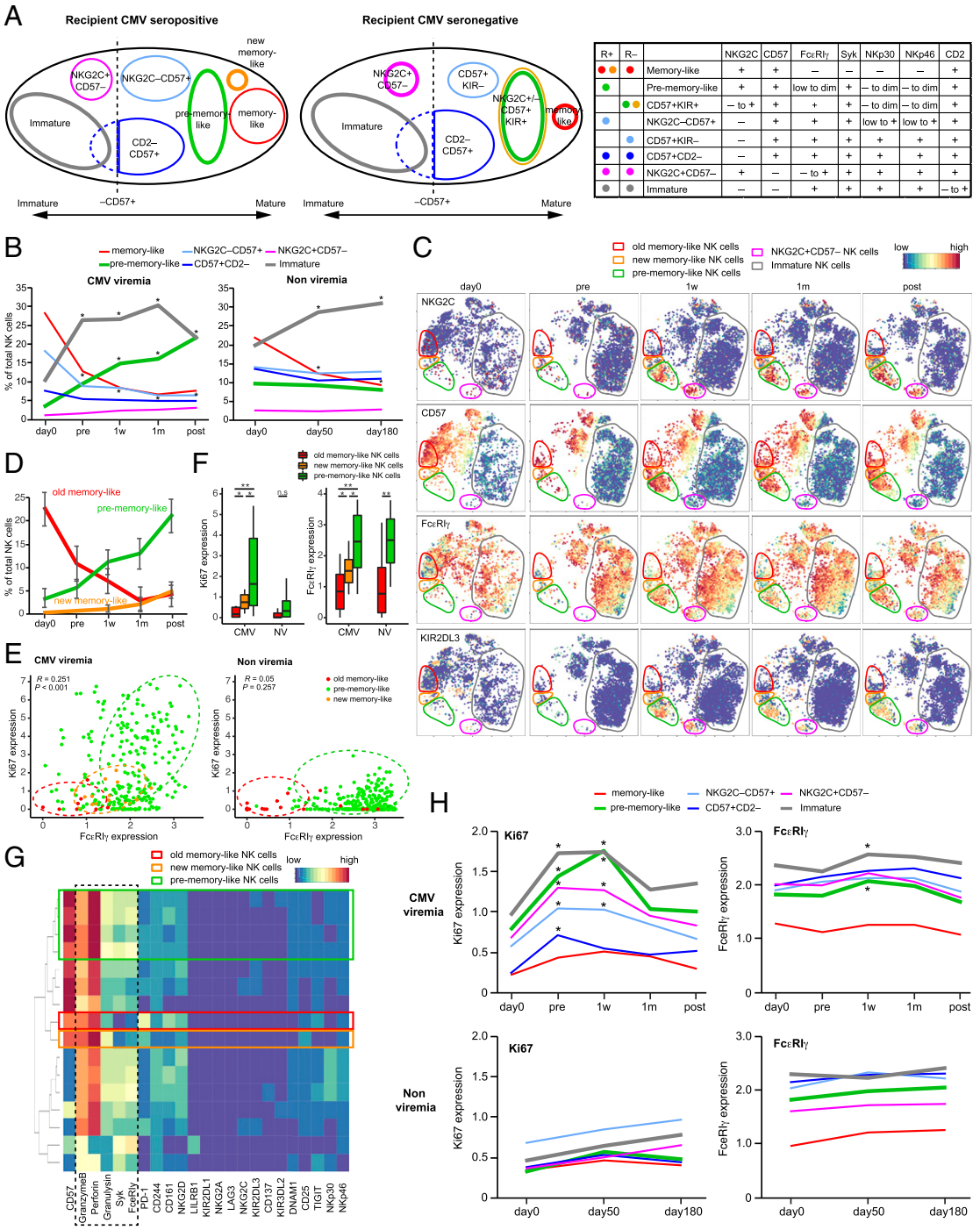

Fig. 3. Longitudinal kinetics of NK cells subsets in R+ patients. (*A*) Schema diagrams shown for NK cell subsets identified by t-SNE analysis in R+ patients (*Left*) and R– patients (*Right*). Bold line-shaped subsets are significantly expanded subsets in CMV viremic patients. The horizontal line indicates maturity as indicated by CD57 expression. The table defines the signature phenotypes representative of each NK cell subset. The colored plots in the table correspond to the subsets in the schema. New memory-like NK cells are observed only in R+ viremic patients and exhibit FcεRIγ$^-$ to low intermediate level between preexisting memory-like and prememory-like NK cells. CD57$^+$KIR$^+$ NK cells in R– patients are a cluster composed of NKG2C$^+$ (green) and NKG2C$^-$ (gold) cells. (*B*) Line graphs showing longitudinal changes of the frequencies of six NK cell subsets. Data represent the average from R+ viremic patients ($n = 5$) and R+ NV patients ($n = 6$). Statistical significance was analyzed with the Student's *t* test, relative to the day 0 time point. (*C*) Representative t-SNE plots showing longitudinal change of phenotypes in an R+ viremic patient. Colored shapes delineate old (preexisting) memory-like (red), new memory-like (orange), prememory-like (green), and NKG2C$^+$CD57$^-$ (pink) NK cells. (*D*) Line graphs showing longitudinal change of the frequencies of the three memory-like NK cells. Data represent the average ± SEM from R+ viremic patients ($n = 3$). (*E*) Representative single-cell scatterplots showing Ki67 and FcεRIγ expression of the three memory-like NK cells. The Pearson product–moment correlation coefficient was used to evaluate the association. (*F*) Box plots showing single-cell Ki67 and FcεRIγ expression of the three memory-like NK cells compiled from R+ viremic ($n = 5$) and R+ NV patients ($n = 6$). (*G*) Heat map showing each marker expression in an R+ viremic patient. Colored boxes indicate marker profiles of the three memory-like NK cells. A dotted line box highlights cytotoxic molecules and intracellular molecules. (*H*) Line graphs showing longitudinal changes of Ki67 and FcεRIγ expression of six NK cell subsets. Data represent the average from R+ viremic patients ($n = 5$) and R+ NV patients ($n = 6$). Statistical significance was analyzed with the Student's *t* test, relative to the day 0 time point. n.s., not significant. *$P < 0.05$; **$P < 0.01$.

cell subsets with different NK marker expression in recipient CMV-seronegative (R–) patients (Fig. 3*A* and *SI Appendix*, Fig. S2). A proportion of R– patients had memory-like NK cells, presumably generated by infections other than CMV, although the size of the population is much smaller compared with R+ patients. Immature NK cells were defined as $NKG2C^{-}CD57^{-}NKp30^{+}NKp46^{+}$ cells regardless of CD2 in R– and R+ patients. Given that $CD57^{+}KIR^{+}$ NK cells express different levels of NKG2C expression on the cell surface, we identified $NKG2C^{+}$ or $NKG2C^{-}$ cells within the $CD57^{+}KIR^{+}$ NK cell population using the single-cell matrix data (*Materials and Methods*). We longitudinally tracked seven NK subsets (memory like, $NKG2C^{+}CD57^{+}KIR^{+}$, $NKG2C^{-}CD57^{+}KIR^{+}$, $CD57^{+}KIR^{-}$, $CD57^{+}CD2$, $NKG2C^{+}CD57^{-}$, and immature) in R– patients. Frequencies of $NKG2C^{+}CD57^{-}$ and $NKG2C^{+}CD57^{+}KIR^{+}$ NK cells with high expression of granulysin increased postviremia, showing a peak up-regulation of Ki67 and FcεRIγ expression at the 1-wk time point (pink and green in Fig. 4). Intriguingly, $NKG2C^{+}CD57^{+}KIR^{+}$ NK cells showed early up-regulation of Ki67 expression at the previremia time point (green in Fig. 4*A*). Reciprocally, $NKG2C^{-}CD57^{+}KIR^{+}$ NK cells decreased at ∼1 wk postinfection (sky blue in Fig. 4*A*). Memory-like NK cells significantly increased at the late postinfection time point (red in Fig. 4). All subsets tended to show up-regulation of FcεRIγ expression over the course of CMV infection. In contrast, there were no significant changes in R– NV patients. Collectively, R– viremic patients showed a dynamic increase of cytotoxic $NKG2C^{+}$ NK cells over CMV viremia along with the accumulation of memory-like NK cells at the late phase of CMV infection.

Single-Cell Inhibitory KIR Repertoire Analysis. A preferential expansion of $NKG2C^{+}CD57^{+}$ NK cells with KIR2DL3 expression has been documented in patients with CMV infection (4, 21). We examined the inhibitory KIR repertoire in kidney transplant patients by evaluating the expression pattern of four inhibitory KIRs within $NKG2C^{+}CD57^{+}$ NK cells, which most frequently express KIRs. Among the 15 different KIR phenotypes that potentially could be stochastically observed, all of the viremic patients having an HLA-C1/C1 or -C1/C2 genotype exclusively displayed a high frequency of single-positive $KIR2DL3^{+}$ NK cells, which was significantly higher in viremic patients than in NV patients no matter the recipient's CMV serostatus (Fig. 5*A*). In addition, memory-like NK cells in viremic patients exhibited a similar KIR composition to $NKG2C^{+}CD57^{+}$ NK cells, showing a high frequency of single-positive $KIR2DL3^{+}$ NK cells (Fig. 5*A*). Longitudinal analysis showed that single-positive $KIR2DL3^{+}$ NK cells dominated the KIR composition over CMV viremia, as memory-like NK cells also exhibited a dynamic change of KIR composition, showing predominant single-positive $KIR2DL3^{+}$ NK cells in viremic patients (Fig. 5 *B* and *C* and *SI Appendix*, Fig. S4 *A* and *B*). Moreover, a high frequency of single-positive $KIR2DL3^{+}$ NK cells was observed in viremic patients, even in those with an HLA-A3, HLA-A11, or HLA-Bw4 haplotype, which have ligands to engage KIR3DL2 or KIR3DL1, respectively (*SI Appendix*, Fig. S4*C*). These data suggest that HLA-C1 is the exclusive factor causing the expansion of single $KIR2DL3^{+}$ NK cells.

Interplay of Different Cytotoxic Lymphocytes in CMV Viremia. As activated $CD8^{+}$ T cells and γδ T cells also frequently express NK receptors, we examined $NKG2C^{+}CD8^{+}$ αβ T cells and γδ T cells in the kidney transplant recipients. t-SNE dimensionality reduction identified $NKG2C^{+}CD8^{+}$ T cells and γδ T cells characterized by coexpression of NKRs and triple cytotoxic molecules (i.e., granzyme B, perforin, and granulysin) (Fig. 6 *A* and *B*). The frequencies of $NKG2C^{+}CD8^{+}$ T cells and triple cytotoxic γδ T cells were higher in viremic patients compared with NV patients (Fig. 6*C*). These data suggest that prememory-like NK cells (R+ patients) or mature $NKG2C^{+}CD57^{+}$ NK cells (R– patients), $NKG2C^{+}CD8^{+}$ T cells, and triple cytotoxic γδ T cells are three different cytotoxic lymphocytes responding to CMV viremia. To demonstrate the interplay of these cytotoxic lymphocytes, we first depicted three-dimensional line graphs of frequencies of these three types of lymphocytes. Two main different patterns were observed; the first is a combinatorial response (solid line circled in Fig. 6 *D*, *Left*), and the second is a skewed response of NK cells or γδ T cells (dotted line circled in Fig. 6 *D*, *Left*). In accordance with the result, these three different cytotoxic lymphocytes exhibited an increase corresponding to patterns of overall lymphocyte frequency (Fig. 6 *D*, *Right*). These data indicate that viremic patients mostly show a combinatorial immune response of different cytotoxic lymphocytes against CMV infection, whereas some patients showed a skewed immune response of selective cytotoxic lymphocytes. Furthermore, R+ viremic patients showed that frequencies and cell counts of the three cytotoxic lymphocytes significantly increased along with a high peak of Ki67 expression at ∼1 wk postviremia (Fig. 6 *E* and *F*). On the other hand, R– viremic patients showed that cell counts of the three cytotoxic lymphocytes significantly increased at 1 mo postviremia, along with a high peak of Ki67 expression at 1 wk postviremia as the frequency of $NKG2C^{+}CD57^{+}$ NK cells showed a significant increase at ∼1 wk postviremia (Fig. 6 *E* and *F*). Such longitudinal changes were not observed in NV patients (*SI Appendix*, Fig. S5). These findings indicate that R+ patients mount a robust immune response to CMV viremia relatively earlier than R– patients.

Longitudinal Change of Anti-Glycoprotein B Antibody Able to Activate CD16 in Renal Transplant Patients. Anti-glycoprotien B (gB) antibodies have been demonstrated to mediate significant protection against CMV infection (22, 23). Mature NK cells express the activating CD16 Fc receptor that mediates ADCC against human IgG1 or IgG3 antibody-coated targets. Further, $CD57^{+}$ and memory-like NK cells induced by CMV infection are the most potent mediators of ADCC function (7, 10, 15). Therefore, we assayed patient sera for the presence of anti-gB antibodies capable of triggering CD16 activation using an *LacZ* CD16 reporter assay. We determined that plasma from CMV viremic patients possesses specific anti-gB antibodies competent to activate CD16 (*SI Appendix*, Fig. S6). A proportion of R+ viremic patients showed increased anti-gB antibody activity, although overall, there was no significant difference between viremic and NV patients (Fig. 7). Intriguingly, elevated CD16-activating anti-gB antibodies were exclusively observed in patients who showed a combinatorial response of cytotoxic lymphocytes (solid line circled in Fig. 6*D*). In contrast, there were no increases in CD16-activating anti-gB antibodies in R– viremic patients. These findings suggest that ADCC via anti-gB antibody was potentially augmented during CMV infection in R+ patients but not in R– patients.

Discussion

In the present study, we addressed NK cell diversity and dynamic kinetics of response in CMV infection by high-dimensional analysis of more than 30 NK cell–associated markers, especially focusing on memory-like NK cells, which have been demonstrated as $NKG2C^{+}$ and/or $FcεRIγ^{-}$ cells in previous studies (15, 24, 25). Dimensionality reduction identified distinct types of NK cells that were mainly characterized by NKG2C, CD57, FcεRIγ, CD2, NKp30, NKp46, and inhibitory KIRs. The longitudinal analysis enabled us to demonstrate not only quantitative changes of each subset but also, cellular relationships among different subsets and in vivo kinetics of the response at the single-cell level over CMV infection. In

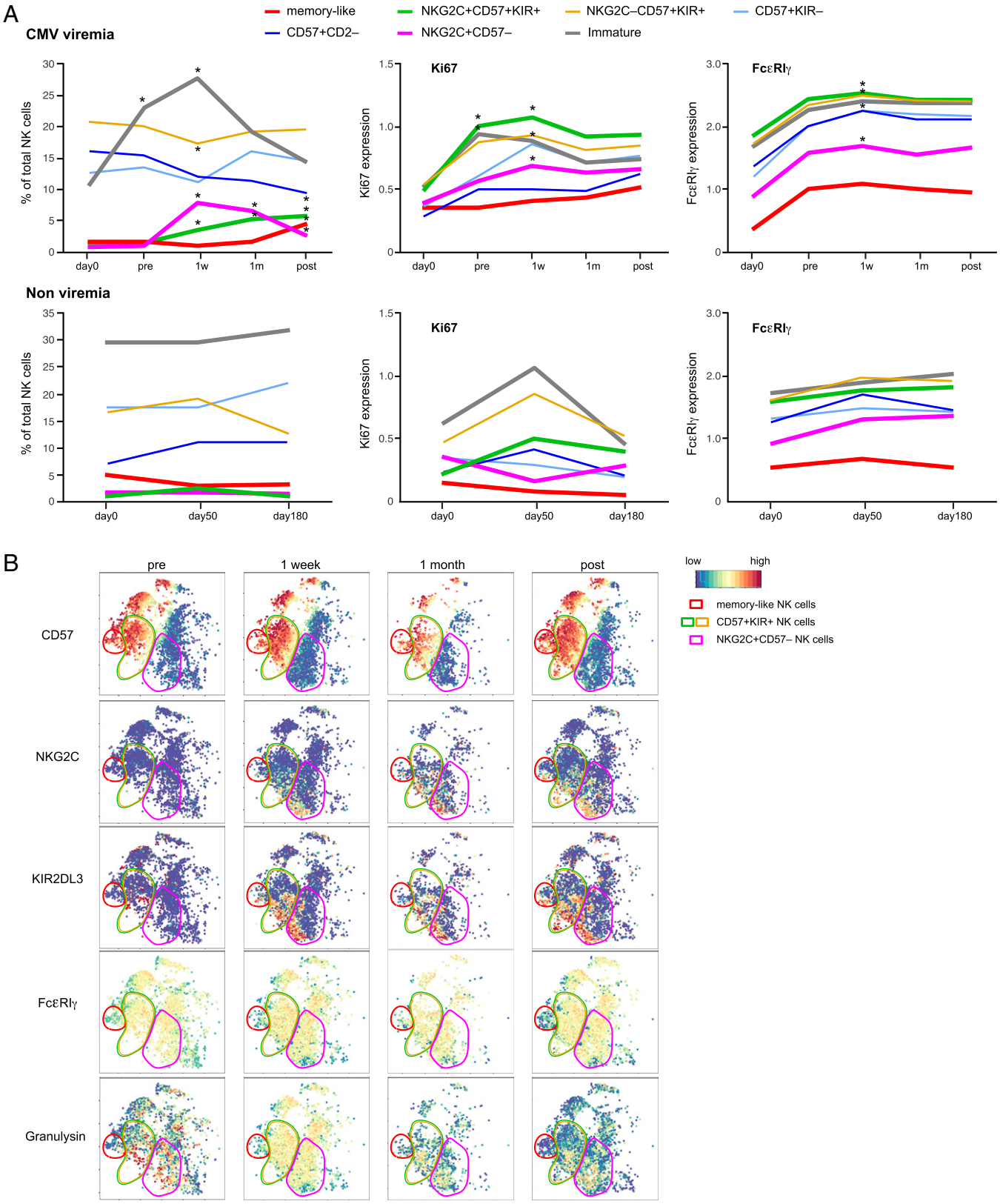

Fig. 4. Longitudinal kinetics of NK cell subsets in R– patients. (*A*) Line graphs showing longitudinal changes of frequencies and Ki67 and FcεRIγ expression of seven NK cell subsets. Data represent the average from R– viremic ($n = 6$) and R– NV patients ($n = 3$). Statistical significance was analyzed with the Student's *t* test, relative to the day 0 time point. (*B*) Representative t-SNE plots showing longitudinal change of phenotypes in an R– viremic patient. Colored shapes delineate memory-like (red), NKG2C^{+}CD57^{-} (pink), and CD57^{+}KIR^{+} NK cells, which are a cluster composed of NKG2C^{+} (green) and NKG2C^{-} (gold). $*P < 0.05$.

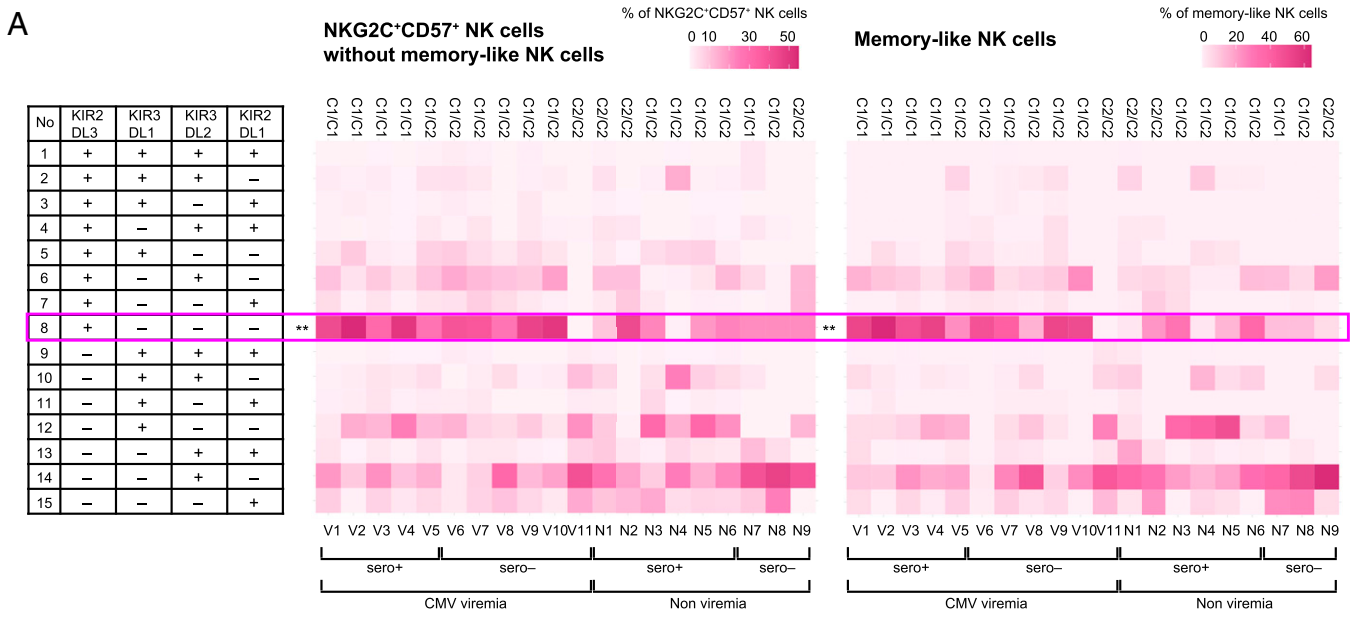

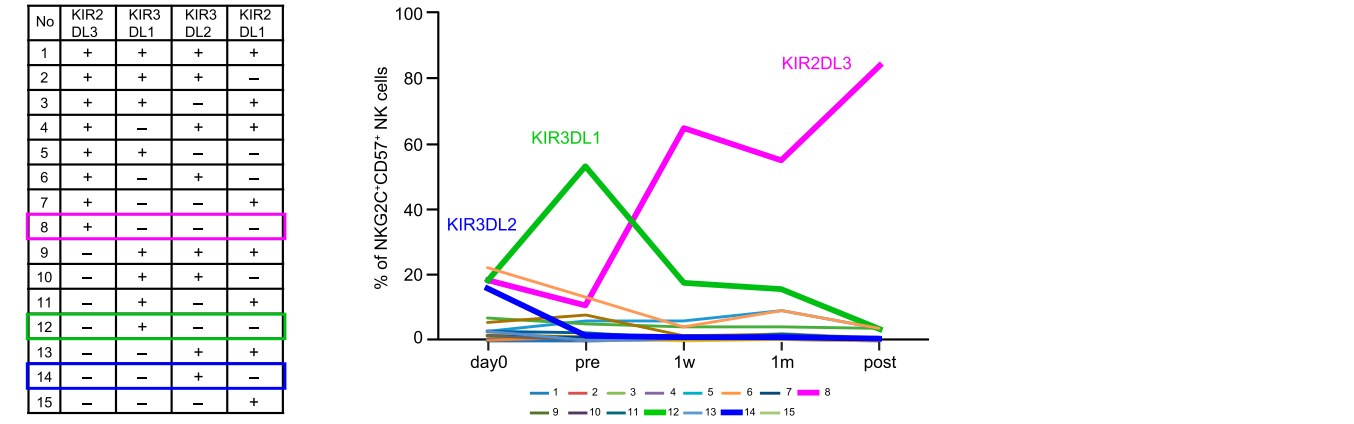

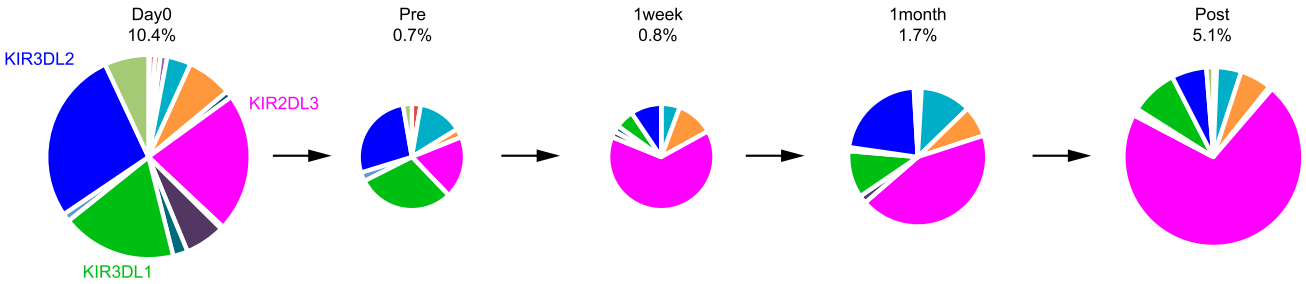

Fig. 5. Single-cell inhibitory KIR repertoire analysis of NK cells. (*A*) Heat map showing the frequencies of NK cells with each inhibitory KIR profile in CD57$^+$ NK cells without memory-like NK cells (*Left*) and with memory-like NK cells (*Right*). Data represent viremic patients (n = 11) and NV patients (n = 9). HLA-C genotypes are described on the top of the heat map. A pink box highlights single KIR2DL3$^+$ NK cells. Comparison of the frequency between viremic patients and NV patients was analyzed with the Student's t test. $^{**}P < 0.01$. (*B*) Line graphs showing longitudinal changes of the frequencies of NK cells with each inhibitory KIR profile in a representative R+ viremic patient. Colored boxes and lines highlight single KIR2DL3$^+$ (pink), KIR3DL1$^+$ (green), and KIR3DL2$^+$ (blue) NK cells. (*C*) Pie charts showing longitudinal changes of inhibitory KIR repertoires of memory-like NK cells in the same patient as in *B*. The value above the pie chart is the percentage of memory-like NK cells in total NK cells at each time point.

addition to NK cells, we identified minor subsets of T cells responding to CMV viremia, which were characterized by expression of NKRs and cytotoxic effector molecules, and demonstrated the interplay of the different cytotoxic lymphocytes against CMV infection.

We observed that preexisting memory-like (NKG2C$^+$ CD57$^+$FcεRIγ$^-$) NK cells in R+ patients decreased and exhibited the lowest Ki67 expression compared with other subsets over viremia. While preexisting memory-like NK cells diminished, we determined that prememory-like NK cells

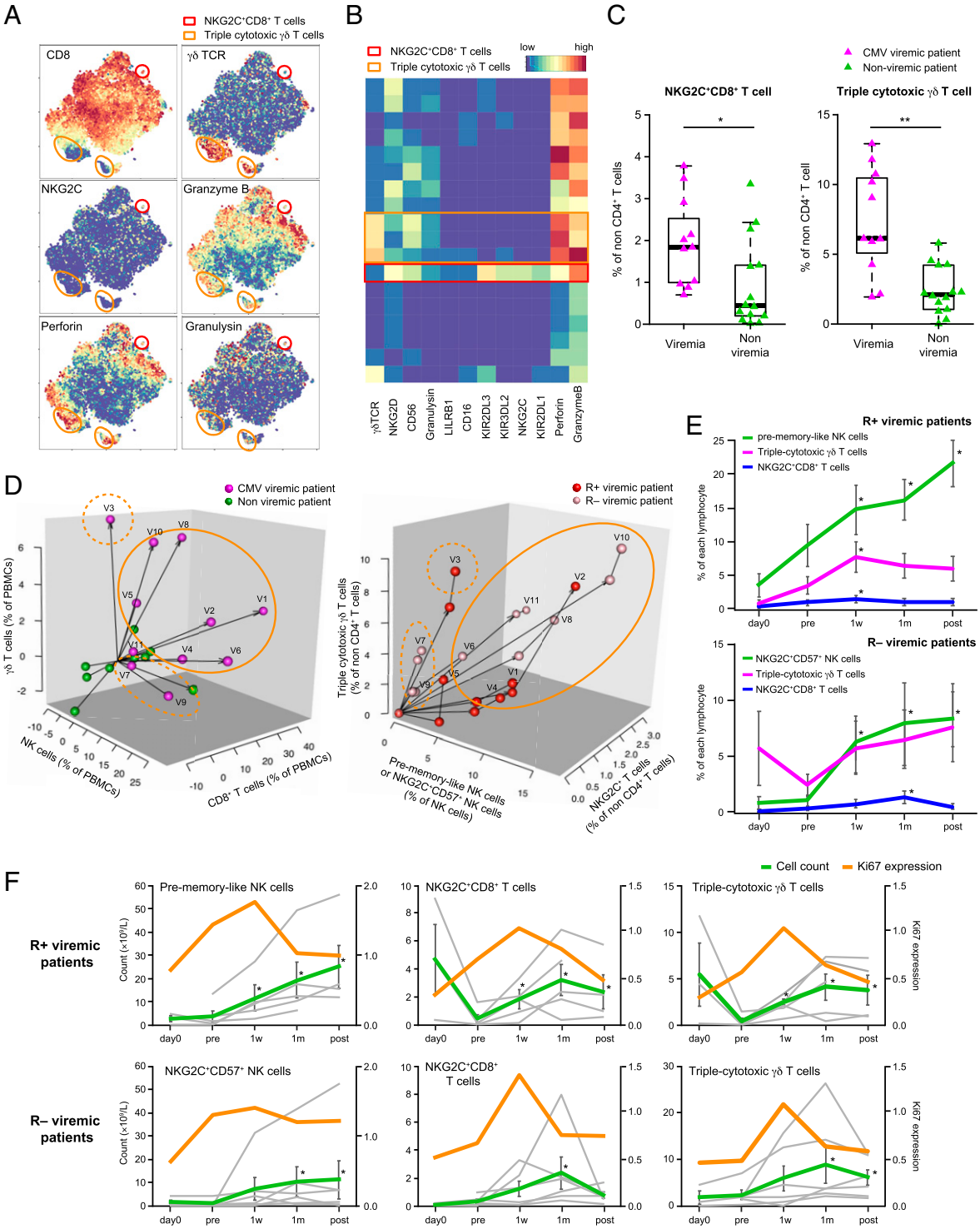

Fig. 6. Interplay of NK cells, $CD8^+$ T cells, and γδ T cells in viremic patients. (*A*) Representative t-SNE plots showing phenotypes of $NKG2C^+$ T cells (red) and triple cytotoxic (granulysin, perforin, granzyme B) γδ T cells (orange). (*B*) Heat map showing marker profiles of $NKG2C^+$ T cells (red) and triple cytotoxic γδ T cells (orange). (*C*) Frequencies of $NKG2C^+CD8^+$ T cells and triple cytotoxic γδ T cells in viremic ($n = 11$) and NV ($n = 9$) patients. Statistical significance was analyzed with the Student's *t* test. (*D*) Three-dimensional line graphs showing longitudinal changes of three different lymphocytes. (*Left*) Frequencies of NK cells, $CD8^+$ T cells, and γδ T cells in viremic (pink) and NV (green) patients. (*Right*) Frequencies of prememory-like NK cells (in R+ patients) or $NKG2C^+CD57^+$ NK cells (in R– patients), $NKG2C^+CD8^+$ T cells, and triple cytotoxic γδ T cells in R+ (red) and R– (white) viremic patients. Variations from previremia to postviremia time points are depicted. Viremic patient identifications are labeled above the plot. (*E*) Line graphs showing longitudinal changes of frequencies of the three different cytotoxic lymphocytes in R+ (*Upper*) and R– (*Lower*) viremic patients. Data represent the average percentage ± SEM from R+ ($n = 5$) and R– ($n = 6$) viremia patients. Statistical significance was analyzed with the Student's *t* test, relative to the day 0 time point. (*F*) Line graphs showing longitudinal changes of cell counts and Ki67 expression of the three different cytotoxic lymphocytes in R+ (*Upper*) and R– (*Lower*) viremic patients. Scales of cell counts and Ki67 expression are described on the left and right sides, respectively. Cell count data represent individual (gray) and the average (green) ± SEM from R+ ($n = 5$) and R– ($n = 6$) viremic recipients. Ki67 expression represents the average (orange). The statistical significance of the mean slope of linear model was evaluated with the Student's *t* test, relative to the previremia time point. $*P < 0.05$; $**P < 0.01$.

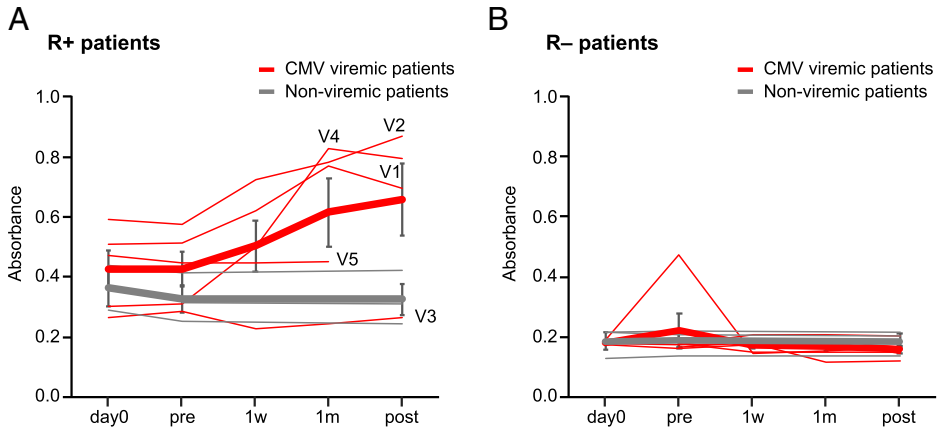

Fig. 7. Longitudinal change of CD16-activating anti-gB antibodies in renal transplant patients. Line graphs showing longitudinal changes of CD16-activating anti-gB antibodies in R+ patients (*Left*) and R– patients (*Right*) as measured by using a CD16 LacZ BWZ cell reporter assay. Patient identifications of R+ viremic patients are labeled. Red lines indicate viremia, and gray lines indicate NV. Bold lines represent the average ± SEM. Data were from R+ viremic ($n = 5$), R+ NV ($n = 6$), R– viremic ($n = 6$), and R– NV ($n = 3$) patients. Statistical significance was analyzed with the Student's *t* test.

($NKG2C^+CD57^+Fc\varepsilon RI\gamma^{low\ to\ dim}$) with a higher cytotoxic profile significantly increased and proliferated (expressing Ki67) over CMV viremia, accompanied by transient up-regulation of FcεRIγ expression. In vitro studies from our laboratory have demonstrated that FcεRIγ expression is up-regulated by cytokine stimulation and positivity correlates with cell proliferation, which support the hypothesis that up-regulation of FcεRIγ is likely due to inflammatory cytokine induction in viremic patients. In addition to cytokine stimulation, interaction with CMV-infected cells might be involved in the in vivo expansion of prememory-like NK cells (26, 27), which is supported by the finding that prememory-like NK cells undergo clonal-like expansion as evidenced by the dominance of single-positive $KIR2DL3^+$ KIR repertoire restriction. Notably, t-SNE analysis demonstrated that newly generated memory-like NK cells merged with prememory-like NK cells accumulated over the viremic time course. The new memory-like NK cells exhibited an intermediate immune profile between preexisting memory-like NK cells and prememory-like NK cells. These data indicate that a proportion of the prememory-like NK cells down-regulate or lose FcεRIγ expression and shift to a memory-like stage over the viremic time course. These prememory-like NK cells appeared to serve as the main population that differentiates into the memory-like stage and have proliferation capacity, resulting in their ability to develop into the $NKG2C^+CD57^+$ NK cell pool with different FcεRIγ expression levels ranging from negative to high in reactivated CMV infection. Importantly, single-cell analysis revealed that $NKG2C^+CD57^+$ NK cells are heterogenous and have different division capabilities and cytotoxic profiles, depending on their FcεRIγ expression level. We have previously demonstrated that ex vivo these $Fc\varepsilon RI\gamma^-$ NK cells have enhanced ADCC functions and proliferation when activated via CD16 (15, 17), whereas our current in vivo study of CMV viremic patients indicated that memory-like NK cells are quite limited compared with other NK cell subsets with respect to proliferation, despite anti-gB antibody production being augmented in R+ viremic patients. These findings indicate that the $Fc\varepsilon RI\gamma^-$ NK cell subset is a very heterogenous population, including quiescent $Fc\varepsilon RI\gamma^-$ NK cells and $Fc\varepsilon RI\gamma^{low}$ NK cells with high proliferative capacity. Our findings and others highlight that FcεRIγ-deficient NK cells, which are termed memory-like, are the long-lived quiescent memory-like population with a terminally differentiated phenotype and limited proliferation capacity (24). Although the physiological role of the memory-like NK cells in humans has not been well studied, the observation that preexisting memory-like NK cells decreased and immature NK cells surged in the peripheral after CMV infection in kidney transplant patients might be linked with NK cell redistribution to peripheral lymphoid and other tissues for immune surveillance, as memory-like NK cells are observed in nonlymphoid organs (24, 28). NK cells might also be affected by the immune-suppressive agents given to transplant patients to prevent graft rejection (29). The patterns of tissue localization of memory-like and prememory-like NK cells in immunocompromised conditions and viral infection should be further analyzed. Collectively, our current study strongly suggests that prememory-like NK cells expressing $Fc\varepsilon RI\gamma^{low\ to\ dim}$ have a high proliferative capability and can be the main progenitors that develop into $NKG2C^+CD57^+$ NK cells with different FcεRIγ expression over CMV infection.

We also identified a very minor population of NK cells at baseline in R– patients with a memory-like phenotypic profile, although the antigen driving this population is unknown. However, we were able to detect significant proliferation of NK cells at later phases of primary CMV infection in R– viremic patients. As is the case in R+ patients, these preexisting memory-like NK cells partially merged into the expanded $NKG2C^+CD57^+$ NK cell subset and exhibited the lowest Ki67 expression among NK cell subsets in R– patients. Moreover, $NKG2C^+CD57^+$ NK cells with single-positive KIR2DL3 expression undergo a clonal-like expansion with progressive KIR repertoire restriction over CMV viremia, accompanied by development of the memory-like NK cell pool with a similar KIR repertoire as $NKG2C^+CD57^+$ NK cells. These data indicate that memory-like NK cells are derived from $NKG2C^+CD57^+$ NK cells and take at least several months to significantly accumulate and constitute the memory-like NK cell pool after primary CMV infection.

In addition to $NKG2C^+$ NK cells, t-SNE analysis identified higher frequencies of $NKG2C^+$ αβ T cells and γδ T cells with NKRs and highly cytotoxic profiles in viremic patients. $NKG2C^+$ T cells and triple cytotoxic γδ T cells demonstrated a peak of Ki67 expression at ∼1 wk postviremia and increased over the time course, indicating that these T cells, as well as prememory-like NK cells, respond to CMV infection. This finding is strengthened by the observation that these cytotoxic lymphocytes did not increase in NV patients. The frequency of $NKG2C^+$ T cells is reported to be high in CMV-seropositive healthy donors and hematopoietic stem cell transplant patients who experienced CMV reactivation (18, 30). As $NKG2C^+$ T cells have the capacity to proliferate in response to different pathogens (31), CMV is one of the pathogens that can drive an

expansion of NKG2C$^+$ T cells. Among γδ T cells, Vγ9^{neg}Vδ2^{pos} T cells have been shown to increase and highly express cytotoxic molecules in CMV infection (32, 33). The triple cytotoxic γδ T cells identified in our study may contain Vγ9^{neg}Vδ2^{pos} T cells considering the similar phenotypes and kinetics observed. NKG2C$^+$ T cells and cytotoxic γδ T cells can be activated via NKRs, which have modulatory functions on proliferation and cytolytic activity, independent of TCR signaling (31, 34). Previous studies and our data imply that NKG2C$^+$ T cells may be driven via innate-like pathways in CMV infection, although some of the NKG2C$^+$ T cells might also harbor CMV-specific T cell receptor (TCR) signaling (35). Intriguingly, R+ viremic patients exhibited a relatively early cellular response of these three cytotoxic lymphocytes compared with R– viremic patients. That indicates that these cytotoxic lymphocytes may have a signature of being susceptible to inflammatory cytokines or a memory-like signature that enables them to quickly respond to CMV rechallenge compared with naıve cells. In fact, NKG2C$^+$ T cells and γδ T cells can be expanded by interleukin-15 (IL-15) (31, 36). Adaptive γδ T cell subsets have been shown to clonally expand in CMV infection (32, 37). Moreover, we observed that a combinatorial interplay of these cytotoxic lymphocytes was found in a proportion of CMV viremic patients. Furthermore, such patients possessed ADCC-competent anti-gB antibodies as shown by an *LacZ* CD16 reporter assay, highlighting that adaptive innate immunity to viral infection is linked with humoral immunity. Considering the preferential CD16 expression on cytotoxic T cells, NKG2C$^+$ T cells, and triple cytotoxic γδ T cells, as well as prememory-like NK cells, anti-gB antibodies might augment these immune responses to CMV infection in R+ patients (17). Further studies are warranted to explore the interplay between innate and adaptive immune cells in viremic patients. Age and genetics may be important modulators, as NKG2C copy number and variants have been predicted to impact immune responses to CMV (38–40). Intriguingly, elevation of anti-gB antibodies was not observed in the R– viremic patients. It is plausible that the initiation of humoral immune responses to primary CMV infection might be suppressed by the immune-suppressive therapy, whereas preexisting antibody-producing cells could be activated even under the immune suppression.

In summary, this study first identifies in depth the in vivo kinetics of NK cell immune responses to primary vs. reactivation of CMV, revealing dynamic changes within the NKG2C$^+$CD57$^+$ NK cell subset depending on FcεRIγ expression over CMV infection in kidney transplant patients. We also identified NKG2C$^+$ T cells and triple cytotoxic γδ T cells, as well as NKG2C$^+$CD57$^+$ NK cells, combinatorially responding to CMV infection. Although this study has a limitation to establish links with clinical outcome because of the enrolled sample size, pretransplant NKG2C$^+$ NK cells have been suggested to have a protective role to CMV viremia (41, 42). Given that all viremic patients, except one patient, overcame viremia and prevented graft rejection, the phenotypic features of cytotoxic lymphocytes in the current study can be related to immune protection against CMV infection rather than immunopathology of graft injury. Prospective studies comprehensively analyzing the in vivo kinetics of cytotoxic lymphocytes in kidney transplant patients, including patients undergoing graft rejection, are warranted to assess immunological features in the clinical management of these patients.

Materials and Methods

More details of the materials and methods are presented in *SI Appendix, Supplemental Materials and Methods*.

Study Population and Clinical Data. We analyzed 83 samples of 27 kidney transplant patients collected over the time course. The longitudinal study consisted of CMV viremic patients ($n = 11$) and NV patients ($n = 9$). Clinical characteristics are summarized in *SI Appendix*, Table S1. Blood sampling in viremic patients had five collecting time points: day 0 (before kidney transplantation), previremia (before viremia), ~1 wk after diagnosis, ~1 mo postviremia, and long-term postviremia (>1 mo after diagnosis). For patients who developed viremia at a late phase of transplantation, we sampled four time points: previremia, ~1 wk, ~1 mo, and late (>1 mo) postviremia. As controls for patients who developed viremia, NV patients had three collecting time points: day 0 and ~90 and ~180 d after transplantation. Individual sampling schedules are described in Fig. 1. Written informed consent was obtained from all the patients. The study was conducted in accordance with the principles of the Helsinki Declaration and was approved by the University of California, San Francisco (UCSF) Institutional Review Board (21-34669).

CMV Protocol and Definitions. Standardized protocols for blood collection, processing, and storage were implemented at UCSF. Recipients were screened routinely to detect CMV viremia by PCR during CMV prophylaxis (0 to 3 mo for R+, 0 to 6 mo for R–) and at the time of discontinuation of CMV prophylaxis (baseline). Scheduled study blood draws were done at baseline and at 12 and 24 mo posttransplantation. In addition, at the time of positive clinical testing results by CMV PCR, samples were collected at 1 ~wk and ~1 mo after positive PCR test results. We selected these time points for profiling as previous studies from our team indicated that CMV-specific CD4$^+$ and CD8$^+$ T cells are detected in the circulation within 7 d after the peak of CMV replication (43). Furthermore, continued T cell responses in the absence of viremia reflect large and long-lasting changes in the memory compartment that justify profiling samples collected at 12 and 24 mo posttransplantation (44). A positive CMV PCR test is defined as a result >137 IU/mL, as specified by the manufacturer. At this relatively low level of CMV PCR positivity, clinicians may sometimes observe a patient without treatment intervention; however, we have chosen this threshold for definition of infection or reactivation because we anticipate that the protective immune response will be assessable at this time point (45).

Statistical Analysis. Comparison of longitudinal changes of lymphocyte subsets was performed using the Student's *t* test. Details are described in figures. Statistical significance was defined as $P < 0.05$ with a two-tailed test. All statistics analyses were performed using the R software 3.6.1 (The R Foundation for Statistical Computing).

Data Availability. All study data are included in the article and/or *SI Appendix*. Mass cytometry data have been deposited on Mendeley Data, https://data.mendeley.com/datasets/fnbvcyf223/1.

ACKNOWLEDGMENTS. We acknowledge the University of California San Francisco Parnassus Flow CoLab (supported by Research Source Identifiers SciCrunch Resolver 018206) for assistance in generating flow/mass cytometry data. The study was supported by NIH Grants U19AI128913 and 1S10OD018040 and NIH Data and Research Center Grant P30 DK063720. K.I. was supported by the Uehara Memorial Foundation.

1. M. Dzabic *et al.*, Intragraft cytomegalovirus protein expression is associated with reduced renal allograft survival. *Clin. Infect. Dis.* **53**, 969–976 (2011).
2. P. Gatault *et al.*, CMV infection in the donor and increased kidney graft loss: Impact of full HLA-I mismatch and posttransplantation CD8(+) cell reduction. *Am. J. Transplant.* **13**, 2119–2129 (2013).
3. S. Lopez-Vergès *et al.*, Expansion of a unique CD57$^+$NKG2Chi natural killer cell subset during acute human cytomegalovirus infection. *Proc. Natl. Acad. Sci. U.S.A.* **108**, 14725–14732 (2011).
4. B. Foley *et al.*, Cytomegalovirus reactivation after allogeneic transplantation promotes a lasting increase in educated NKG2C+ natural killer cells with potent function. *Blood* **119**, 2665–2674 (2012).
5. B. Foley *et al.*, Human cytomegalovirus (CMV)-induced memory-like NKG2C(+) NK cells are transplantable and expand in vivo in response to recipient CMV antigen. *J. Immunol.* **189**, 5082–5088 (2012).
6. M. Della Chiesa *et al.*, Phenotypic and functional heterogeneity of human NK cells developing after umbilical cord blood transplantation: A role for human cytomegalovirus? *Blood* **119**, 399–410 (2012).
7. S. Lopez-Vergès *et al.*, CD57 defines a functionally distinct population of mature NK cells in the human CD56dimCD16+ NK-cell subset. *Blood* **116**, 3865–3874 (2010).
8. N. K. Björkström *et al.*, Expression patterns of NKG2A, KIR, and CD57 define a process of CD56dim NK-cell differentiation uncoupled from NK-cell education. *Blood* **116**, 3853–3864 (2010).

9. D. W. Hendricks *et al.*, Cutting edge: NKG2C(hi)CD57+ NK cells respond specifically to acute infection with cytomegalovirus and not Epstein-Barr virus. *J. Immunol.* **192**, 4492–4496 (2014).
10. N. K. Björkström, A. Svensson, K. J. Malmberg, K. Eriksson, H. G. Ljunggren, Characterization of natural killer cell phenotype and function during recurrent human HSV-2 infection. *PLoS One* **6**, e27664 (2011).
11. S. H. Lee *et al.*, Susceptibility to mouse cytomegalovirus is associated with deletion of an activating natural killer cell receptor of the C-type lectin superfamily. *Nat. Genet.* **28**, 42–45 (2001).
12. A. O. Dokun *et al.*, Specific and nonspecific NK cell activation during virus infection. *Nat. Immunol.* **2**, 951–956 (2001).
13. M. G. Brown *et al.*, Vital involvement of a natural killer cell activation receptor in resistance to viral infection. *Science* **292**, 934–937 (2001).
14. J. C. Sun, J. N. Beilke, L. L. Lanier, Adaptive immune features of natural killer cells. *Nature* **457**, 557–561 (2009).
15. T. Zhang, J. M. Scott, I. Hwang, S. Kim, Cutting edge: Antibody-dependent memory-like NK cells distinguished by FcRγ deficiency. *J. Immunol.* **190**, 1402–1406 (2013).
16. H. Schlums *et al.*, Cytomegalovirus infection drives adaptive epigenetic diversification of NK cells with altered signaling and effector function. *Immunity* **42**, 443–456 (2015).
17. J. Lee *et al.*, Epigenetic modification and antibody-dependent expansion of memory-like NK cells in human cytomegalovirus-infected individuals. *Immunity* **42**, 431–442 (2015).
18. M. Gumá *et al.*, Imprint of human cytomegalovirus infection on the NK cell receptor repertoire. *Blood* **104**, 3664–3671 (2004).
19. V. Pitard *et al.*, Long-term expansion of effector/memory Vdelta2-gammadelta T cells is a specific blood signature of CMV infection. *Blood* **112**, 1317–1324 (2008).
20. T. Crough, R. Khanna, Immunobiology of human cytomegalovirus: From bench to bedside. *Clin. Microbiol. Rev.* **22**, 76–98 (2009).
21. V. Béziat *et al.*, NK cell responses to cytomegalovirus infection lead to stable imprints in the human KIR repertoire and involve activating KIRs. *Blood* **121**, 2678–2688 (2013).
22. W. J. Britt, L. Vugler, E. J. Butfiloski, E. B. Stephens, Cell surface expression of human cytomegalovirus (HCMV) gp55-116 (gB): Use of HCMV-recombinant vaccinia virus-infected cells in analysis of the human neutralizing antibody response. *J. Virol.* **64**, 1079–1085 (1990).
23. A. Bootz *et al.*, Protective capacity of neutralizing and non-neutralizing antibodies against glycoprotein B of cytomegalovirus. *PLoS Pathog.* **13**, e1006601 (2017).
24. K. H. Kim *et al.*, Phenotypic and functional analysis of human NK cell subpopulations according to the expression of FcεRIγ and NKG2C. *Front. Immunol.* **10**, 2865 (2019).
25. A. Rölle, P. Brodin, Immune adaptation to environmental influence: The case of NK cells and HCMV. *Trends Immunol.* **37**, 233–243 (2016).
26. A. Rölle *et al.*, IL-12-producing monocytes and HLA-E control HCMV-driven NKG2C+ NK cell expansion. *J. Clin. Invest.* **124**, 5305–5316 (2014).
27. M. Gumá *et al.*, Expansion of CD94/NKG2C+ NK cells in response to human cytomegalovirus-infected fibroblasts. *Blood* **107**, 3624–3631 (2006).
28. P. Dogra *et al.*, Tissue determinants of human NK cell development, function, and residence. *Cell* **180**, 749–763.e13 (2020).
29. M. D. Bunting *et al.*, GVHD prevents NK-cell-dependent leukemia and virus-specific innate immunity. *Blood* **129**, 630–642 (2017).
30. R. Sottile *et al.*, Human cytomegalovirus expands a $CD8^+$ T cell population with loss of *BCL11B* expression and gain of NK cell identity. *Sci. Immunol.* **6**, eabe6968 (2021).
31. S. J. Balin *et al.*, Human antimicrobial cytotoxic T lymphocytes, defined by NK receptors and antimicrobial proteins, kill intracellular bacteria. *Sci. Immunol.* **3**, eaat7668 (2018).
32. S. Ravens *et al.*, Human γδ T cells are quickly reconstituted after stem-cell transplantation and show adaptive clonal expansion in response to viral infection. *Nat. Immunol.* **18**, 393–401 (2017).
33. H. Kaminski *et al.*, Characterization of a unique γδ T-cell subset as a specific marker of cytomegalovirus infection severity. *J. Infect. Dis.* **223**, 655–666 (2021).
34. J. Kim *et al.*, Innate-like cytotoxic function of bystander-activated $CD8^+$ T cells is associated with liver injury in acute hepatitis A. *Immunity* **48**, 161–173.e5 (2018).
35. L. E. Gamadia *et al.*, Differentiation of cytomegalovirus-specific CD8(+) T cells in healthy and immunosuppressed virus carriers. *Blood* **98**, 754–761 (2001).
36. H. H. Van Acker *et al.*, Interleukin-15 enhances the proliferation, stimulatory phenotype, and antitumor effector functions of human gamma delta T cells. *J. Hematol. Oncol.* **9**, 101 (2016).
37. M. S. Davey *et al.*, The human $V\delta2^+$ T-cell compartment comprises distinct innate-like $V\gamma9^+$ and adaptive $V\gamma9^-$ subsets. *Nat. Commun.* **9**, 1760 (2018).
38. A. Muntasell *et al.*, NKG2C zygosity influences CD94/NKG2C receptor function and the NK-cell compartment redistribution in response to human cytomegalovirus. *Eur. J. Immunol.* **43**, 3268–3278 (2013).
39. M. R. Goodier *et al.*, Rapid NK cell differentiation in a population with near-universal human cytomegalovirus infection is attenuated by NKG2C deletions. *Blood* **124**, 2213–2222 (2014).
40. Q. Zhang *et al.*, COVID-STORM Clinicians; COVID Clinicians; Imagine COVID Group; French COVID Cohort Study Group; CoV-Contact Cohort; Amsterdam UMC Covid-19 Biobank; COVID Human Genetic Effort; NIAID-USUHS/TAGC COVID Immunity Group, Inborn errors of type I IFN immunity in patients with life-threatening COVID-19. *Science* **370**, eabd4570 (2020).
41. D. Redondo-Pachón *et al.*, Adaptive NKG2C+ NK cell response and the risk of cytomegalovirus infection in kidney transplant recipients. *J. Immunol.* **198**, 94–101 (2017).
42. M. Ataya *et al.*, Pretransplant adaptive NKG2C+ NK cells protect against cytomegalovirus infection in kidney transplant recipients. *Am. J. Transplant.* **20**, 663–676 (2020).
43. A. S. Chong, M. L. Alegre, The impact of infection and tissue damage in solid-organ transplantation. *Nat. Rev. Immunol.* **12**, 459–471 (2012).
44. R. M. van Ree *et al.*, Latent cytomegalovirus infection is an independent risk factor for late graft failure in renal transplant recipients. *Med. Sci. Monit.* **17**, CR609–CR617 (2011).
45. H. T. Kuo, X. Ye, M. S. Sampaio, P. Reddy, S. Bunnapradist, Cytomegalovirus serostatus pairing and deceased donor kidney transplant outcomes in adult recipients with antiviral prophylaxis. *Transplantation* **90**, 1091–1098 (2010).